The Mechanical Stability of Immunoglobulin and Fibronectin III Domains in the Muscle Protein Titin Measured by Atomic Force Microscopy

Matthias Rief,* Mathias Gautel,# Alexander Schemmel,* and Hermann E. Gaub*
*Lehrstuhl für Angewandte Physik, Ludwig Maximilians Universität München, 80799 München, and #EMBL, Biological Structures Division, Postfach 102209, 69012 Heidelberg, Germany

ABSTRACT The domains of the giant muscle protein titin (connectin) provide interaction sites for other sarcomeric proteins and fulfill mechanical functions. In this paper we compare the unfolding forces of defined regions of different titin isoforms by single-molecule force spectroscopy. Constructs comprising six to eight immunoglobulin (Ig) domains located in the mechanically active I-band part of titin are compared to those containing fibronectin III (Fn3) and Ig domains from the A-band part. The high spatial resolution of the atomic force microscope allows us to detect differences in length as low as a few amino acids. Thus constructs of different lengths may be used as molecular rulers for structural comparisons with other modular proteins. The unfolding forces range between 150 and 300 pN and differ systematically between the constructs. Fn3 domains in titin exhibit 20% lower unfolding forces than Ig domains. Fn3 domains from tenascin, however, unfold at forces only half those of titin Fn3 domains. This indicates that the tightly folded titin domains are designed to maintain their structural integrity, even under the influence of stretching forces. Hence, at physiological forces, unfolding is unlikely unless the forces are applied for a long time (longer than minutes).

INTRODUCTION

The giant muscle protein titin (also known as connectin) (Maruyama et al., 1977; Wang et al., 1979) is a modular protein consisting mainly of structurally similar Ig and Fn3 domains. A single titin molecule spans the whole range between the M-line and the Z-disc (>1 μm) in striated muscle (Fürst et al., 1988). In the A-band titin is firmly attached to the thick filaments, whereas in the I-band, titin acts as a reversible spring when the sarcomere is passively stretched (reviewed in Maruyama, 1997). The molecular mechanism of this elasticity has been elucidated in several recent studies. Even the unfolding of Ig domains has been suggested as a source of elasticity (Erickson, 1994). However, antibody labeling experiments have since shown that the main contribution to the extension of titin under external force stems from a nonmodular sequence rich in proline, glutamate, valine, and lysine (PEVK segment) (Gautel et al., 1996; Linke et al., 1996). This finding was supported by single-molecule force measurements where titin molecules were stretched and domain unfolding was observed only at forces high above the physiological range (Kellermayer et al., 1997; Rief et al., 1997a; Tskhovrebova et al., 1997). These studies also showed that domain unfolding is a time-dependent process, and that the unfolding force hence depends on the velocity at which the force is applied.

Titin occurs in both cardiac and skeletal isoforms (Labeit et al., 1995; Wang et al., 1991). Fig. 1 shows the I-band region and the beginning of the A-band region of these isoforms. The main differences reside in the size of their I-band regions, where the skeletal isoforms have up to 53 additional Ig domains and a much longer PEVK region (Labeit and Kolmerer, 1995). In this paper we present single-molecule force spectroscopy data on the stability of recombinant constructs from different parts of titin. The constructs (marked *blcak* in Fig. 1) where chosen from the constitutive I-band part of titin (ConIg, I27-I34), the skeletal-specific Ig insert (SkIg, Sk47-Sk53), the beginning of the A-band (ConFn, I48-I54), and the C-zone in the center of the thick filament (AFn, A60-A65). The aim of this study is to elucidate the distribution of mechanical stability along the more than 200 Ig and Fn3 domains in titin by investigating representative sets of domains.

EXPERIMENTAL

Protein expression

For expression of titin fragments, multidomain fragments were phased according to the stability criteria for titin immunoglobulin domains established by Politou et al. (1994). The modules are numbered according to the nomenclature of Labeit and Kolmerer (1995); amino acid numbers in human cardiac titin (EMBL X90568) are 13758–14353 (A60-A65), 7170–7872 (I48-I54), 5237–5947 (I27-I34), and 4445–5120 (skeletal titin EMBL X90569, Ig domains sk47-sk53). Titin fragments were amplified by polymerase chain reaction from primary human muscle cDNA and expressed in *Escherichia coli* with the pET expression system (Studier et al., 1990). The plasmids were verified by restriction analysis and DNA end sequencing to contain the correct titin fragments. An N-terminal histidine$_6$ tag (encoded by the pET vectors) and two C-terminal tandem cysteine residues (encoded by the synthetic 3′ oligonucleotides) were fused in frame to the titin fragments. The plasmids were transformed into BL21[DE3] cells (Studier et al., 1990). Protein expression was induced in cultures grown to OD_{600} = 0.6 at 37°C, 200 rpm, by 0.1 mM IPTG for 4 h as described (Freiburg and Gautel, 1996; Politou et al., 1994). The solubly expressed His$_6$-tagged protein was purified from cytosolic supernatants by metal chelate affinity chromatography (LeGrice and Grüninger-Leitch, 1990) on Ni^{2+}-NTA agarose (Qiagen, Germany), following the manufacturer's instructions. Further

Received for publication and in final form

Address reprint requests to Dr. Matthias Rief, Lehrstuhl für Angewandte Physik, Ludwig Maximilians Universität München, Amalienstrasse 54, 80799 München, Germany. Tel.: 0000000000; Fax: 00000000000; E-mail: 0000000000000.

0006-3495/98/12/3008/07 $2.00

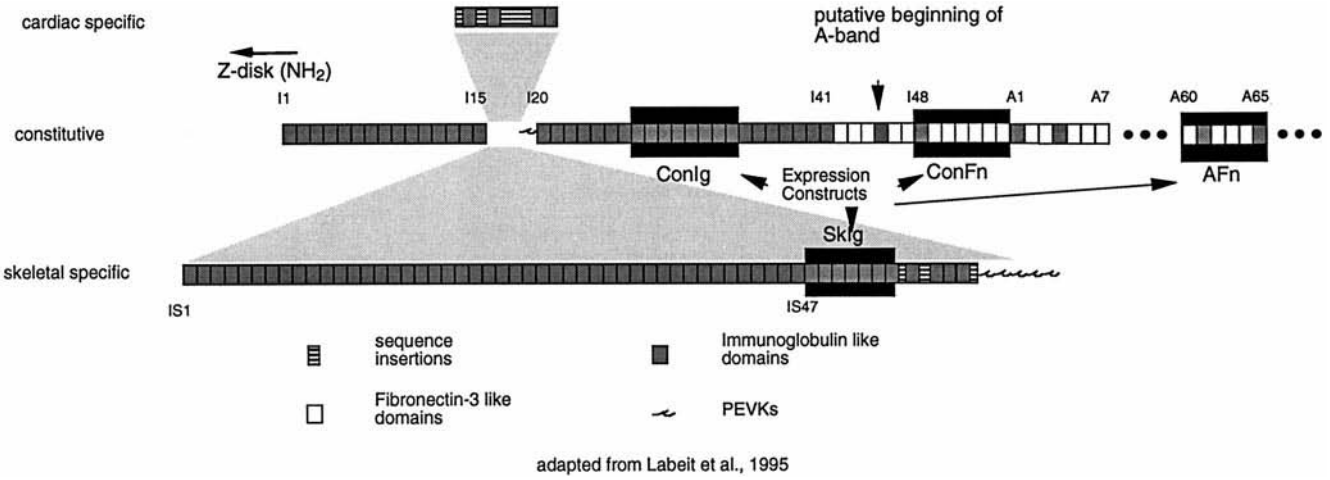

FIGURE 1 Domain structure of I-band titin including the beginning of the A-band part. The skeletal and the cardiac titin isoforms consist of a constitutive part that is identical in the two forms. Between domains I15 and I20 titin is differentially spliced, with the skeletal form having 53 more Ig domains and a much longer PEVK segment. The recombinant constructs used in the experiments are marked in black.

purification was achieved for I48-I54 and sk47-sk53 by anion exchange chromatography on a monoQ 20/5 column (Pharmacia, Sweden) in 20 mM Tris-Cl, 1 mM EDTA, 5 mM dithiothreitol (pH 8.0) and elution gradients of 0–500 mM NaCl. The proteins were equilibrated and stored in 20 mM potassium phosphate (pH 7), 150 mM NaCl, 1 mM EDTA, 1 mM NaN_3, and 5 mM dithiothreitol (to keep the cysteine tag reduced) at protein concentrations of 1–5 mg/ml. Storage in this buffer for several weeks was possible without degradation or aggregation, as judged by sodium dodecyl sulfate-polyacrylamide gel electrophoresis (SDS-PAGE) (Laemmli, 1970). The functionality of the C-terminal tandem-cysteine tag was confirmed by atomic force microscopy (AFM) measurements (as successful attachment to the gold surface) and by nonreducing SDS-PAGE after exposure to excess atmospheric oxygen or 3% H_2O_2 (v/v) for >2 h, which showed the formation of dimers not observed in reducing gels (not shown). Immediately before AFM measurements, the proteins were passed over a NAP-10 desalting column (Pharmacia); equilibrated in 20 mM potassium phosphate (pH 7), 150 mM NaCl, 1 mM EDTA to remove the reducing agents; subsequently adjusted to working concentrations (50 μg/ml); and immediately used for coating of gold-covered glass slides.

The recombinant construct TenFn comprising 15 Fn3 domains from human tenascin was a generous gift from Harold P. Erickson and corresponds to the TenfnALL construct desribed by Aukhil et al. (1993).

Sample preparation

Proteins were allowed to adsorb to a freshly evaporated gold surface from a 50-μl drop of a 50 μg/ml solution in phosphate-buffered saline (PBS) (pH 7.4, 150 mM NaCl). After the incubation process (10 min) the sample was rinsed with PBS. Force measurements were carried out in PBS as well.

Force measurements

Force measurements were carried out with a custom-built AFM. Commercially available silicon nitride cantilevers (Digital Instruments, Santa Barbara, CA) were used as force sensors (k_C = 60–100 mN/m). No special treatment was applied to the tips. Spring constants were determined for each cantilever by measuring the amplitude of its thermal noise (Butt and Jaschke, 1995; Florin et al., 1995; Hutter and Bechhoefer, 1994). To detect relative differences in the unfolding forces between the different constructs without calibration error, traces on different constructs were measured with the same cantilever. All force curves for which pulling speeds are not explicitly given were recorded at a piezo extension velocity of 0.5 μm/s.

Fig. 2 shows a force spectroscopic experiment performed on a recombinant construct of a modular protein. For simplicity a construct comprising only four Ig domains is sketched. The construct is anchored to the gold surface via two carboxy-terminal cysteines. The AFM tip is carefully brought into contact with the protein-coated surface, and the proteins are picked up by the tip via adsorption. It has been shown in various studies that adsorption can lead to very high connecting forces (>700 pN) (Li et al., 1998; Rief et al., 1997a,b). The pickup can occur at any domain along the construct. Subsequently, the mechanical stability of the domains spanning the gap between tip and gold surface can be probed. The sequential unfolding of the domains results in a sawtooth pattern as depicted in Fig. 2. In a previous study (Rief et al., 1997a) it could be shown that the slope leading up to each peak is mainly determined by the elasticity of the already unfolded polypeptide. At the peak force the weakest of the folded domains in the chain unfolds in an all-or-none event adding an additional stretch of unraveled polypeptide to the chain. Hence the absolute value of the peak force marks the unfolding force of a domain, and the spacing to

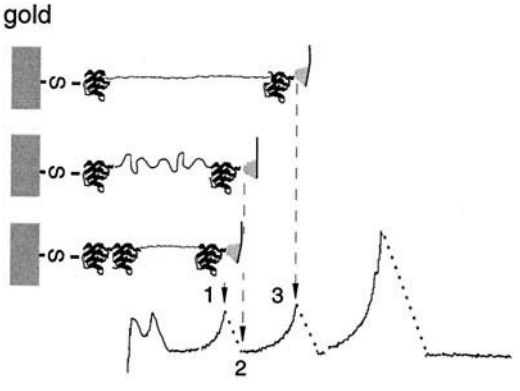

FIGURE 2 Scheme of an unfolding experiment. The recombinant constructs are bound to a gold surface via carboxy-terminal cysteines. The protein is picked up by an AFM tip and stretched until a domain unfolds (*1*). The domains unfold in an all-or-none event, adding an additional stretch of polypeptide to the already unfolded chain (*2*). The polypeptide chain is now stretched again until the next domain unfolds (*3*). From the peak values of the traces the unfolding force of the domains can be measured. From the spacing of the peaks the number of aminoacids folded in the domains can be deduced.

the following peak reflects the gain in length during a transition from the folded configuration to the fully unraveled polypeptide strand and can be correlated to the number of amino acids folded in this domain.

It has been shown that cysteine binds strongly to gold surfaces (Dakkouri et al., 1996). However, it cannot be ruled out that the titin constructs may also attach to the gold surface via nonspecific adsorption. Previous studies have shown that immobilization of proteins by adsorption can also lead to high attachment forces (Oberhauser et al., 1998; Rief et al., 1997a). In fact, the TenFN construct investigated in this study and in the study by Oberhauser et al. (1998) lacks cysteine tags but is still accessible to force spectroscopic experiments. Because in this case both the attachment to the surface and the pickup by the AFM tip can occur along any domain in the chain, the number of domains probed in the experiment is in most traces below the total number of domains in the construct. It turned out that the presence of the carboxy-terminal cysteine tag increases the incidence of traces reflecting the unfolding of the maximum number of domains. All traces shown in this study are selected to show a maximum number of unfolding peaks.

Worm-like chain fits

To model the force versus extension characteristics of the unfolded polypeptide, the interpolation formula introduced by Bustamante et al. (1994) was used:

$$F(x) = \frac{k_B \cdot T}{p}\left(\frac{1}{4 \cdot (1 - x/L)^2} - \frac{1}{4} + \frac{x}{L}\right) \qquad (1)$$

The persistence length p describes the polymer stiffness, k_B is Boltzmann's constant, L is the contour length, and T is the temperature. Fig. 3 shows a release trace of a previously unfolded stretch of the TenFn construct. The two black lines are WLC force versus extension curves with two different persistence lengths and contour lengths. The solid line is for a persistence length of $p = 0.4$ nm, as in Rief et al. (1997a). For the dotted line, p was chosen as 0.8 nm. This value describes the elasticity of the unfolded polypeptide strand best in a force range of 0–50 pN. To model the elasticity in the complete force range of up to 200 pN, $p = 0.4$ nm seems to be more appropriate. Nevertheless, there are deviations, especially in the low-force regime. This reflects the problems in describing by a single parameter p the complicated elasticity of a real polymer that is dominated by entropic as well as enthalpic contributions due to bond angle deformations. There is also definitely a need for improved polymer elasticity models describing the force extension traces at high forces above 50 pN.

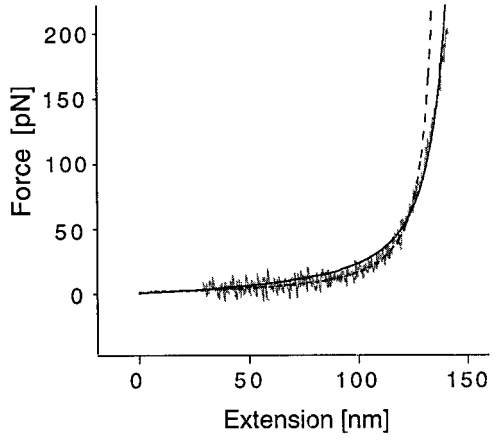

FIGURE 3 Release trace of a previously unfolded stretch of the TenFn construct. The curve shows the elasticity of the unfolded polypeptide over a large range of forces (0–200 pN). The black curves are WLC fits to the data. The dashed curve is drawn for a persistence length $p = 0.8$ nm and the solid curve for $p = 0.4$ nm.

For the purpose of the current study, where a model is needed to obtain values for changes in contour length and correlate these to the number of amino acids in a domain, the WLC model with a persistence length of 0.4 nm is satisfactory. If one wants to make a comparison to persistence lengths obtained in, e.g., optical tweezers experiments (forces < 50 pN), the value of the dotted curve in Fig. 3 (0.8 ± 0.2 nm) has to be used. There is good agreement with a single-component WLC fit applied to stretching curves of native titin, where a value of 0.76 nm was obtained (Tskhovrebova et al., 1997).

Monte Carlo simulation

To model the measured speed dependence of the unfolding forces a simple Monte Carlo simulation is carried out as follows (details will be given in Rief et al., *Phys. Rev. Lett.*, in press). The force generated by stretching the polypeptide chain is calculated using the worm-like chain (*1*) with a persistence length p of 0.4 nm. The probability of unfolding for each of the domains was calculated as $p = \Delta t/\tau$ ($\Delta t \ll \tau$), where Δt is the polling interval and τ is the lifetime of a domain given by (Bell, 1978; Evans et al., 1991)

$$\tau(F) = \tau_0 \cdot e^{(-F \cdot x_u)/k_B T} \qquad (2)$$

τ_0 is the lifetime of a domain at zero force, F is the applied force, and x_u is the width of the linearized unfolding potential. The simulation is carried out by stretching the polypeptide chain by a small amount; computing the resulting force with the WLC model; calculating the domain unfolding probability for that force; and then polling the domains with a random number generator to define their status. With each unfolding event the contour length L of the polypeptide strand is increased by $\Delta L = 28$ nm. From repeated trials, we compute the average unfolding force at different pulling speeds. By fitting the calculated speed dependence to the measured data, values for τ_0 and x_u can be obtained. As can be seen from Eq. 2, the accuracy in determining τ_0 is much lower than the accuracy of x_u. This is due to the fact that $\tau(F)$ depends only linearly on τ_0 but exponentially on x_u. For τ_0 only the order of magnitude can be obtained.

RESULTS

Fig. 4 shows two representative traces taken on each of the recombinant constructs. The superposition on the right shows that within the same construct all traces exhibit exactly the same spacing of the peaks and only small statistical fluctuations in the unfolding force. A persistent feature in all traces is that the unfolding forces within each construct tend to rise from the first to the last peak by nearly a factor of 2. The average force, however, differs only slightly between the different constructs. As shown in Table 1, the most stable construct is ConIg, with an average unfolding force of 237 pN. The weakest domains are contained in ConFn and AFn, whose average unfolding force is 200 pN and 180 pN, respectively. For comparison, two traces recorded on a recombinant construct comprising 15 Fn3 domains from human tenascin (TenFn) are also shown (Fig. 4 and Table 1). Although structurally highly homologous to the ConFn domains, the TenFn domains unfold at only half the forces of the titin constructs. The average unfolding force for TenFn is 113 pN.

The superposition of traces from ConIg, SkIg, and ConFn in Fig. 5 reveals another difference between the constructs: an increasing mismatch between the sawteeth of the respective traces can be observed. This mismatch is due to the

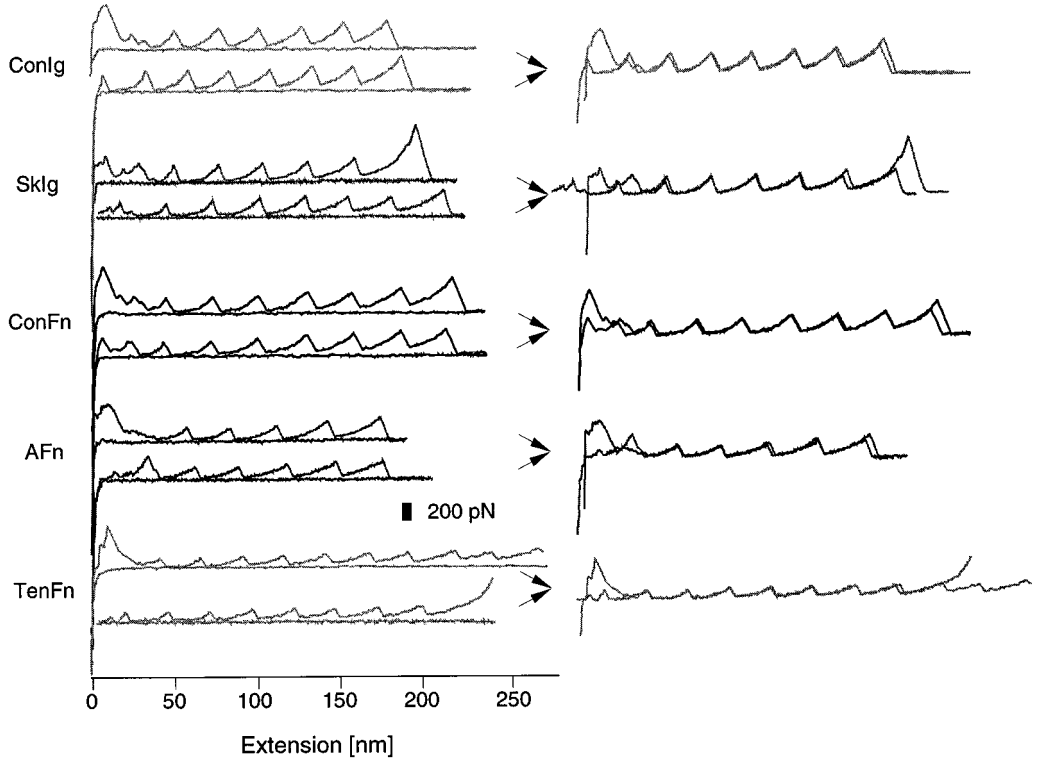

FIGURE 4 Force versus extension traces taken on the four different constructs from titin and an additional construct from tenascin comprising 15 fibronectin III domains. In the left column two traces of each construct are shown. A superposition of these two traces is shown in the right column. The traces on tenascin show less than the maximum number of possible peaks. As explained in the Experimental section, the pickup of the construct can occur at any domain along the construct. In this case only 8–10 of the 15 possible domains were located between tip and substrate.

difference in length of the domains between the constructs. A quantitative analysis where the slope leading up to the peaks in each construct was fitted using the worm-like chain model (*1*) led to the average changes in contour length ΔL listed in Table 1. As an example, the fits to a curve taken on ConFn are shown in Fig. 6. The values for ΔL are directly correlated to the average number of amino acids per domain in each construct.

The dependence of the unfolding forces on the pulling speed for titin and tenascin is presented in Fig. 7. The titin data, recorded on a stretch of native titin, were taken from Rief et al. (1997a). The tenascin data were recorded at 10 different speeds. The average number of domains unfolded in each trace was five. An analysis based on a simple Monte Carlo simulation as described in the Experimental section resulted in the dashed lines in Fig. 7. A fit of the simulation to the data yielded a width of the unfolding potential of x_u = 3 ± 1 Å for titin and 5.5 ± 1 Å for the tenascin domains. The lifetime of the domains at zero force, τ_0, was determined to be 30,000 ± 10,000 s for both molecules.

DISCUSSION

The data in Figs. 4 and 5 reveal that the unfolding forces of titin domains are generally statistically distributed over the molecule. This can be seen from the fact that all unfolding records show peak forces rising from 150 to 300 pN within one construct. There do not seem to be assemblies of domains that show closely homogeneous mechanical properties. The average stabilities, on the other hand, show subtle but consistent differences (~20%) between A-band Fn3 domains and I-band Ig domains, and even a smaller difference between skeletal specific and constitutive Ig do-

TABLE 1 Comparison of the constructs

	Conlg	Sklg	ConFn	AFn	Ten Fn
Avg. no. of aas per domain	89	95.7	99.8	100	90.2
ΔL	28.2 nm	29.8 nm	31 nm	31.5 nm	28.6 nm
Avg. unfolding force	237 pN	210 pN	200 pN	180 pN	113 pN

Summary of the measured properties of all constructs. The first row shows the average number of amino acids for the domains contained in the respective construct. ΔL is the average gain in length of the polypeptide backbone due to the unfolding of the domains. The last row shows the average unfolding force of the domains in each construct.

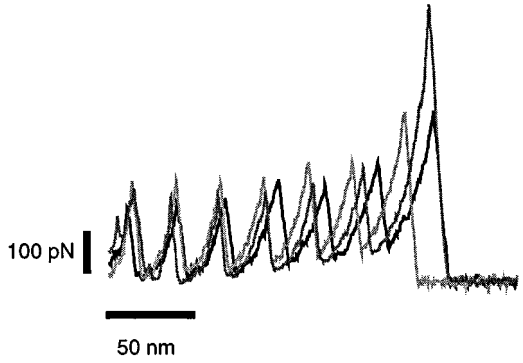

FIGURE 5 Superposition of traces from the three different titin constructs, ConIg (*light gray*), SkIg (*dark gray*), and ConFn (*black*). The increasing mismatch between the three sawtooth patterns reflects the difference in the number of amino acids that are folded in the various domains. It can also be seen that the unfolding forces of ConFn are lower than those of the Ig constructs.

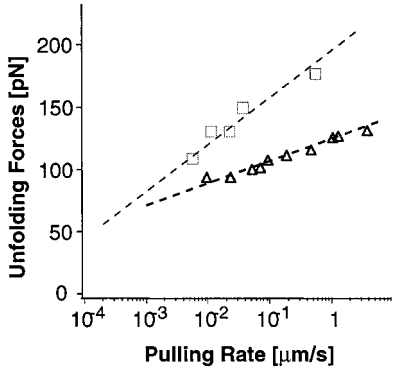

FIGURE 7 Dependence of the unfolding force on the pulling speed for native titin (□) and for the TenFn construct (△). The data for native titin are taken from Rief et al. (1997a). The dashed lines are the results of the computer simulation with x_u = 3 Å and x_u = 5.5 Å, respectively. τ_0 was chosen as 30,000 s.

mains. This short-range variability is in good agreement with a study by Politou et al. (1995) where the thermal and chemical stabilities of Ig and Fn3 domains were examined. In this study, a variation in folding free energy of up to a factor of 3 was detected within the four domains I27-I30 also contained in the construct ConIg of this study.

Generally, however, the comparison of mechanical and thermal stability is not straightforward: whereas thermal stability is mainly determined by the difference in free energy between the folded and unfolded states, mechanical stability depends on the complicated multidimensional energy landscape of protein folding (Frauenfelder et al., 1991). This is especially important for understanding the 50% difference in mechanical stability observed between ConFn and TenFn (see Fig. 4). In contrast to this difference, the numbers given by Clarke et al. (1997) for the melting temperature and the equilibrium free energy of the third Fn3 domain in human tenascin do not differ much from those given for titin Ig and Fn3 domains by Politou et al. (1995). Novel information can be obtained by directly measuring the mechanical stability. This can be seen from Fig. 7, where the dependence of the unfolding force on the pulling velocity is shown: in addition to the unfolding forces, the analysis of the slope of the displayed curves yields an estimate for the width of the unfolding potential x_u mentioned in Eq. 2. Compared to titin (x_u = 3 Å), the value of x_u = 5.5 Å for TenFn is higher by nearly the same factor as the average unfolding force F is lower. Thus the product $F \cdot x_u$, which has the dimensions of energy, leads to approximately the same value for the titin and tenascin domains. Because an important part of the function of titin in muscle is mechanical, the mechanical stability of the domains is a natural measure for this function. The observation of high unfolding forces in all titin constructs compared to TenFn thus suggests a compelling interpretation: titin domains seem to have evolved specifically to keep their structural integrity even under the influence of external forces. Physiological forces of less than a few tens of piconewtons (Linke et al., 1996) are far below the lowest forces that led to domain unfolding in the present study.

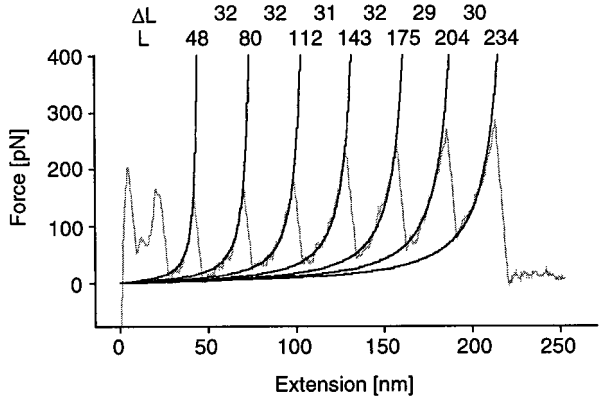

FIGURE 6 A trace taken on ConFn together with WLC-fits according to Eq. 2. The numbers above the fits are the actual contour length L of the fits and the gain in contour length upon unfolding of a domain ΔL.

The data on whole native titin molecules and the TenFn construct in Fig. 7 show that the unfolding forces depend on the rate at which the force is applied. This rate dependence leads to the following seeming discrepancy, which can be resolved using the kinetic view of the unfolding process expressed in Eq. 2.

In an experiment of Tshkovrebova et al. (1997) a strand of native skeletal titin comprising some 70 domains was stretched stepwise with optical tweezers. The relaxation of the force due to domain unfolding was recorded within 1.5 s before the next extension step was applied to the protein. Traces like the one shown in Fig. 8 *a* were obtained. It has been argued (Erickson, 1997) that there appears to be a discrepancy between the unfolding forces of ~200 pN reported in the present study and the plateau of 70–80 pN to which the force decreases within 1.5 s after each step in the optical tweezer experiment. In Fig. 8 *b* the Monte Carlo simulation described in the Experimental section using the

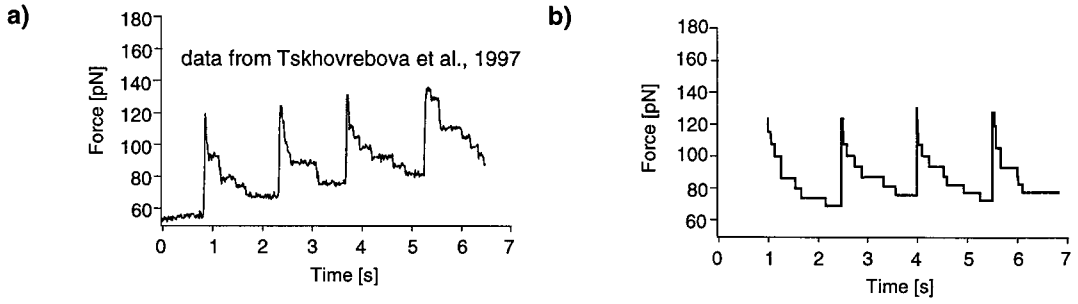

FIGURE 8 (*a*) A step relaxation experiment performed with a strand of titin comprising 80 Ig domains. The data are taken from Tskhovrebova et al. (1997). A force of 120 pN was applied to the titin strand, and then the extension was kept constant for 1.5 s and the relaxation of the force due to the unfolding of individual domains was recorded. This cycle was repeated four times. The force relaxes to 60–80 pN. (*b*) Simulation of this experiment using the parameters derived from AFM experiments. The simulation reproduces the experiment very well. AFM and optical tweezers measurements led to the same result.

same parameters (x_u = 3 Å, τ_0 = 30,000 s) that describe well the AFM experiments was used to model the optical tweezers experiment. The congruence between data and experiment is very good and shows that the seeming difference in unfolding forces is due just to the different time scales at which the experiments were performed.

The consequence of Eq. 2 is obvious: unfolding forces are meaningful only in connection with the time scale of the measurements. Even a small stretching force will eventually lead to unfolding if it is applied long enough. It has to be emphasized, however, that refolding can only be neglected if the applied forces are higher than the range of forces where refolding can happen. At extreme physiological stretching forces of more than 10 pN, refolding will not occur, because the refolding force has been reported by Kellermayer et al. (1997) to be 2.5 pN. Equation 2 can now be used to calculate the time it will take for any single domain within 100 domains to unfold at a constant stretching force of 10 pN. At this force Eq. 2 gives a lifetime for a single domain of 15,000 s. The fact, however, that we consider 100 domains, each with a lifetime of 15,000 s, reduces the time needed for any of these domains to unfold by a factor of 100. This means that in a titin segment of 100 domains, extended constantly at 10 pN, unfolding will start after 3 min of stretch.

The strong time dependence of the unfolding forces, together with the high domain stability at fast pulling rates, has implications for muscle elasticity: during a normal contraction cycle, lasting only for a few seconds, domain unfolding is unlikely even at very high physiological forces. In this case the passive elasticity will be dominated by the mechanical properties of the nonmodular PEVK segment. This is in good agreement with the titin elasticity models derived from antibody labeling studies (Gautel and Goulding, 1996; Linke et al., 1996). If muscle is stretched over a long time (longer than minutes), domain unfolding can occur and may prevent the sarcomere from irreversible damage, as proposed by Rief et al. (1997a). At high (unphysiological) overstretches, however, irreversible detachment of titin from the A-band as a mechanism competitive with domain unfolding has also been reported (Wang et al., 1991).

Variations in average domain stability, as we report them here for the reference domains of titin, will influence the statistical half-lives in the given titin segment; it is obvious that the constitutive Ig domains with the highest average unfolding forces are the least likely to unfold. This explains why ultrastructural studies of isometrically extended heart or skeletal muscle, monitoring the length of the constitutive Ig segments comprising 13–21 Ig domains, detected no evidence of domain unfolding (Bennett et al., 1997; Gautel and Goulding, 1996; Gautel et al., 1996). Because the unfolding of even a single domain will result in great drops in isometric tension (Tskhovrebova et al., 1997), the reversible "sacrifice" of one or very few domains will reduce the unfolding probability of further domains on a reasonably short time scale (several minutes). In agreement with the experimental data obtained in optical tweezers experiments (Tskhovrebova et al., 1997) and the simulations derived from AFM data in Fig. 8, unfolding is most likely to immediately follow a stepwise extension, and consequently domain unfolding becomes less likely the longer the observation time. If domains unfold in isometric extension experiments, this effect will thus be most readily detectable in the differentially spliced skeletal Ig domains and within observation times of few minutes, after which the system will approach equilibrium.

Fig. 5 points toward a very intriguing conceptual feature of force spectroscopy with modular proteins: the molecular vernier. As in a caliper, the sensitivity of the measurement may be significantly increased by comparing two proteins with domains that differ slightly in length in the same measurement. A minute difference is amplified by the modularity; the pattern mismatch grows proportionally to the number of domains. As can be seen in Fig. 5 and Table 1, a difference in length between ConIg and TenFn as small as a single amino acid can be reliably detected. More and more force spectroscopy data on different kinds of domains will provide a collection of characteristic molecular "rulers" with different "fingerprints," and the unfolding forces, to-

gether with the precise spacing of the peaks, could make force spectroscopy a useful tool of molecular biology.

CONCLUSION

The domains of titin vary in biological function but share remarkably high mechanical unfolding forces when compared to other modular proteins like tenascin. The constitutively expressed Ig domains, comprising most of the cardiac titin I-band, show the highest average unfolding forces. Differentially spliced skeletal Ig domains differ in their molecular fingerprint in the AFM by their longer length and slightly lower average unfolding forces. Domains involved in extensive protein-protein interactions, like those of the myosin-associated A-band region of titin, show the lowest unfolding forces, possibly reflecting their stabilization by the binding forces of their respective interactions. Single-molecule force spectroscopy provides a unique tool for the high-resolution study of mechanically active modular proteins and a deepened understanding of local functions within such proteins.

We thank Harold P. Erickson for the preparation of the TenFn construct and Julio M. Fernandez for helpful discussions.

REFERENCES

Aukhil, I., P. Joshi, Y. Yan, and H. P. Erickson. 1993. Cell- and heparin-binding domains of the hexabrachion arm identified by tenascin expression proteins. *J. Biol. Chem.* 268:2542–2553.

Bell, G. I. 1978. Models for the specific adhesion of cells to cells. *Science.* 200:618–627.

Bennett, P. M., T. E. Hodkin, and C. Hawkins. 1997. Evidence that the tandem Ig domains near the end of the muscle thick filament form an inelastic part of the I-band titin. *J. Struct. Biol.* 120:93–104.

Bustamante, C., J. F. Marko, E. D. Siggia, and S. Smith. 1994. Entropic elasticity of λ-phage DNA. *Science.* 265:1599–1600.

Butt, H.-J., and M. Jaschke. 1995. Calculation of thermal noise in atomic force microscopy. *Nanotechnology.* 6:1–7.

Clarke, J., S. J. Hamill, and C. M. Johnson. 1997. Folding and stability of a fibronectin type III domain of human tenascin. *J. Mol. Biol.* 270: 771–778.

Dakkouri, A. S., D. M. Kolb, R. Edelstein-Shima, and D. Mandler. 1996. Scanning tunneling microscopy study of L-cysteine on Au(111). *Langmuir.* 12:2849–2852.

Erickson, H. P. 1994. Reversible unfolding of fibronectin type III and immunoglobulin domains provides the structural basis for stretch and elasticity of titin and fibronectin. *Proc. Natl. Acad. Sci. USA.* 91: 10114–10118.

Erickson, H. P. 1997. Stretching single protein molecules: titin is a weird spring. *Science.* 276:1090–1092.

Evans, E., D. Berk, and A. Leung. 1991. Detachment of agglutinin bonded red blood cells. I. Forces to rupture molecular point attachments. *Biophys. J.* 59:838–848.

Florin, E. L., M. Rief, H. Lehmann, M. Ludwig, C. Dornmair, V. T. Moy, and H. E. Gaub. 1995. Sensing specific molecular interactions with the atomic force microscope. *Biosens. Bioelectron.* 10:895–901.

Frauenfelder, H., A. G. Sligar, and P. G. Wolynes. 1991. The energy landscapes and motions of proteins. *Science.* 1598–1603.

Freiburg, A., and M. Gautel. 1996. A molecular map of the interactions of titin and myosin-binding protein C: implications for sarcomeric assembly in familial hypertrophic cardiomyopathy. *Eur. J. Biochem.* 235: 317–323.

Fürst, D. O., M. Osborn, R. Nave, and K. Weber. 1988. The organization of titin filaments in the half-sarcomere revealed by monoclonal antibodies in immunoelectron microscopy; a map of ten non-repetitive epitopes starting at the Z line extends close to the M line. *J. Cell Biol.* 106: 1563–1572.

Gautel, M., and D. Goulding. 1996. A molecular map of titin/connectin elasticity reveals two different mechanisms acting in series. *FEBS Lett.* 385:11–14.

Gautel, M., E. Lehtonen, and F. Pietruschka. 1996. Assembly of the cardiac I-band region of titin/connectin: expression of the cardiac-specific regions and their relation to the elastic segments. *J. Muscle Res. Cell Motil.* 17:449–461.

Hutter, J. L., and J. Bechhoefer. 1994. Calibration of atomic-force microscope tips. *Rev. Sci. Instrum.* 64:1868–1873.

Kellermayer, M. S., S. B. Smith, H. L. Granzier, and C. Bustamante. 1997. Folding-unfolding transitions in single titin molecules characterized with laser tweezers. *Science.* 276:1112–1116.

Labeit, S., and B. Kolmerer. 1995. Titins, giant proteins in charge of muscle ultrastructure and elasticity. *Science.* 270:293–296.

Laemmli, U. K. 1970. Cleavage of structural proteins during the assembly of the head bacteriophage T4. *Nature.* 227:680–685.

LeGrice, S. F. J., and F. Grüninger-Leitch. 1990. Rapid purification of homodimer and heterodimer HIV-1 reverse transcriptase by metal chelate affinity chromatography. *Eur. J. Biochem.* 187:307–314.

Li, H., M. Rief, F. Oesterhelt, and H. E. Gaub. 1998. Single-molecule force spectroscopy on xanthan by AFM. *Adv. Materials.* 10:316–319.

Linke, W. A., M. Ivemeyer, N. Olivieri, B. Kolmerer, J. C. Rüegg, and S. Labeit. 1996. Towards a molecular understanding of the elasticity of titin. *J. Mol. Biol.* 261:62–71.

Maruyama, K. 1997. Connectin/titin, giant elastic protein of muscle. *FASEB J.* 11:341–345.

Maruyama, K., S. Matsubara, R. Natori, Y. Nonomura, S. Kimura, K. Ohashi, F. Murakami, S. Handa, and G. Eguchi. 1977. Connectin, an elastic protein of muscle: characterization and function. *J. Biochem.* 82:317–337.

Oberhauser, A. F., P. E. Marszalek, H. P. Erickson, and J. M. Fernandez. 1998. The molecular elasticity of the extracellular matrix protein tenascin. *Nature.* 393:181–185.

Politou, A. S., M. Gautel, C. Joseph, and A. Pastore. 1994. Immunoglobulin-type domains of titin are stabilized by amino-terminal extension. *FEBS Lett.* 352:27–31.

Politou, A. S., D. J. Thomas, and A. Pastore. 1995. The folding and stability of titin immunoglobulin-like modules, with implications for the mechanism of elasticity. *Biophys. J.* 69:2601–2610.

Rief, M., M. Gautel, F. Oesterhelt, J. M. Fernandez, and H. E. Gaub. 1997a. Reversible unfolding of individual titin immunoglobulin domains by AFM. *Science.* 276:1109–1112.

Rief, M., F. Oesterhelt, B. Heymann, and H. E. Gaub. 1997b. Single molecule force spectroscopy on polysaccharides by AFM. *Science.* 275:1295–1297.

Studier, F. W., A. H. Rosenberg, J. J. Dunn, and J. W. Dubendorff. 1990. Use of T7 RNA polymerase to direct expression of cloned genes. *Methods Enzymol.* 185:60–89.

Tskhovrebova, L., J. Trinick, J. A. Sleep, and R. M. Simmons. 1997. Elasticity and unfolding of single molecules of the giant muscle protein titin. *Nature.* 387:308–312.

Wang, K., R. McCarter, J. Wright, J. Beverly, and R. Ramirez-Mitchell. 1991. Regulation of skeletal muscle stiffness and elasticity by titin isoforms: a test of the segmental extension model of resting tension. *Proc. Natl. Acad. Sci. USA.* 88:7101–7105.

Wang, K., J. McClure, and A. Tu. 1979. Titin: major myofibrillar components of striated muscle. *Proc. Natl. Acad. Sci. USA.* 76:3698–3702.